Chapter 5
Characterization of Polymer

The characterization of polymer is a vital part of polymer technology. Once the polymers are designed and synthesized, we need to characterize them chemically to confirm their chemical structures and to evaluate their properties for physical behaviors and actual usages [1].

5.1 Instruments and Testing Methods for Polymer Characterization

There are numerous instruments available for polymer characterization. For the chemical structure characterization of polymers, infrared spectroscopy (IR), Raman spectroscopy, ultraviolet–visible spectroscopy (UV–Vis), nuclear magnetic resonance spectroscopy (NMR), and electron spin resonance spectroscopy (ESR) are commonly used. To study the structure and morphology of polymers, X-ray diffraction (XRD), transmission electron microscopy (TEM), scanning electron microscopy (SEM), and atomic force microscopy (AFM) are used in general. The thermal properties of polymers are characterized by differential scanning calorimetry (DSC), dynamic mechanical analysis (DMA), thermal mechanical analyzer (TMA), and thermal gravimetric analysis (TGA). The mechanical properties of polymers are studied by Instron. We will discuss the principle of each instrument briefly, and then show examples how the polymers are being characterized by different instrument.

In industry, there are many standard testing methods being developed to characterize polymers by international organization and different countries. The international standard organization (ISO) standard is an international effort to develop standard test. In the USA, there is the American Society for Testing and Materials (ASTM) to set up the standard. The British Standards Institute (BSI) establishes British's standards. In Taiwan, the standards of testing methods (CNS) follow other countries' standards. Please refer to the tests whenever you are in need. They are available by purchasing them through each standard organization. You can also find them in most of libraries and Taiwan Standard Bureau. We will not discuss them here.

W.-F. Su, *Principles of Polymer Design and Synthesis*,
Lecture Notes in Chemistry 82, DOI: 10.1007/978-3-642-38730-2_5,
© Springer-Verlag Berlin Heidelberg 2013

5.2 Characterization of Chemical Structures of Polymers

5.2.1 Chemical Reaction Method

To determine the chemical structure of polymers through chemical reaction method is a low cost analysis but needs large sample size (>1 gram). For example, the location of head to head structure (1, 2-diol) on polyvinyl alcohol can be determined by the following reaction.

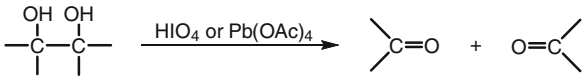

The structures of polydienes can be determined via ozonolysis. Ozonolysis of natural rubber, for example, followed by hydrolysis of the intermediate ozonide under reductive conditions, yields 4-ketopentanal, which establishes the structure as the head-to-tail 1, 4-addition polymer of 2-methyl-1, 3-butadiene (isoprene).

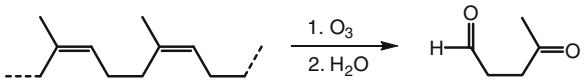

The amount of double bonds in the polymer chain can be determined by the bleaching of known amount of iodine solution through the addition of reaction of iodine to the double bonds.

5.2.2 Infrared Spectroscopy

The infrared spectra of polymers are resulted from the different IR absorption of chemical bonds (vibrational transition) of polymers upon irradiation of IR [1]. The amount of vibrational transition can be expressed by

$$v = \frac{1}{2\pi C}\sqrt{\frac{k}{M_x M_y/(M_x + M_y)}} \tag{5.1}$$

where v is stretching frequency in cm^{-1}, M_x, M_y the masses of two atoms involved in stretching, (grams), C is the velocity of light, 2.998×10^{10} cm/s, and k is force constant, dynes/cm; single bond (5×10^5 dynes/cm), double bond (10×10^5 dynes/cm), and triple bond (15×10^5 dynes/cm). Infrared frequency is usually expressed in units of *wavenumber*, defined as the number of waves per centimeter. Ordinary instruments scan the range of about 700–5,000 cm^{-1}. This frequency range corresponds to energies of about 2–12 kcal/mol. This amount of energy is sufficient to affect bond vibrations (motions such as bond stretching or bond bending) but is appreciably less than would be needed to break bonds. These motions are illustrated in Fig. 5.1.

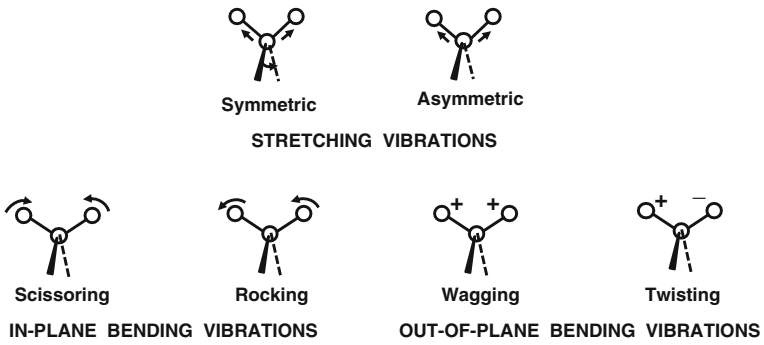

Fig. 5.1 Vibrations of a group of atoms (+ and − signify vibrations perpendicular to the plane of the paper) [2]

Particular types of bonds of organic molecule usually stretch within certain rather narrow frequency ranges which are very useful to determine the chemical structure of molecule. Table 5.1 gives the ranges of stretching frequencies for some bonds commonly found in organic molecules.

The chemical structures of unknown polymers can be recognized mostly through their specific IR absorption frequency. However, their exact chemical structures cannot deduce from IR spectra only, unless they can be compared with known data or from the IR spectra of their monomers. Figure 5.2 shows the difference of IR spectra between polyimide and its chemical repeating unit model compound is at the p-substituting linkage between the aromatic structure of monomers with C–H bending at 650–900 cm^{-1}.

Table 5.1 Infrared stretching frequencies of some typical bonds [2]

Bond type	Class compound	Frequency range (cm^{-1})
Single bonds to hydrogen	alkanes	2,850–3,000
	alkenes and aromatic	3,030–3,140
	alkynes	3,300
	alcohols and phenols	3,500–3,700 (free)
		3,200–3,500 (hydrogen-bonded)
	carboxylic acids	2,500–3,000
	amines	3,200–3,600
	thiols	2,550–2,600
Double bonds	alkenes	1,600–1,680
	imines, oximes	1,500–1,650
	aldehydes, ketones, esters, acids	1,650–1,780
Triple bonds	alkynes	2,100–2,260
	nitriles	2,200–2,400
Subsitute aromatics	ortho	750
	para	830
Halide	C–F	2,962–2,853
	C–Cl	800–600
	C–Br	600–500

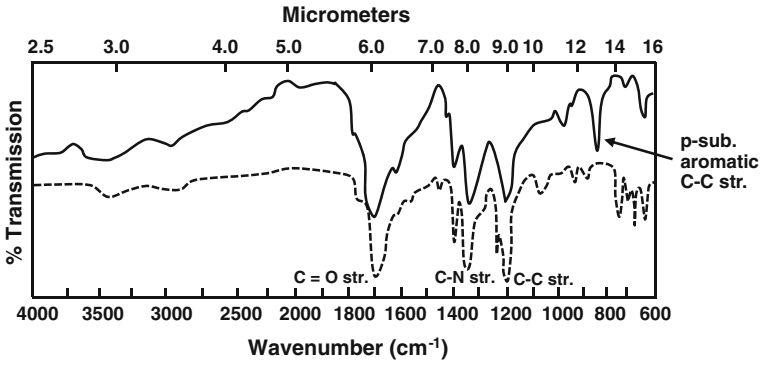

Fig. 5.2 Infrared spectrum (KBr pellets) of polyimide (—) and model compound (- - - -) [3]

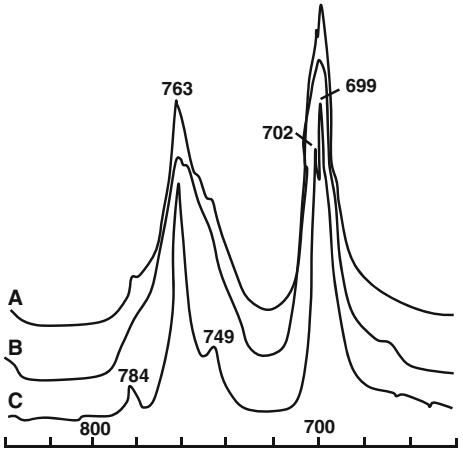

Fig. 5.3 Fourier transform infrared spectra of isotactic polystyrene in the 640–840 cm^{-1} region: (A) semicrystalline; (B) amorphous; and (C) the difference spectrum obtained by subtracting B from A [3]

The IR of isotactic polystyrene can be obtained by subtracting the spectrum of amorphous polystyrene from the spectrum of semicrystalline polystyrene as shown in Fig. 5.3. A well-defined sharp absorption is revealed which indicates the benzene rings are "frozen" into relatively specific conformations in the crystalline state.

5.2.3 Raman Spectroscopy

Like IR spectroscopy, Raman derives from vibrational transitions in molecules. When visible light impinges on molecules, the light is scattered. The frequency of the scattered light varies according to the vibrational modes of the scattering molecules. This referred to as the *Raman effect.* Whereas IR absorption spectra are indicative of unsymmetric bond stretching and bending, the Raman effect responds to the symmetric vibrational modes. Polar groups of a molecule give the most

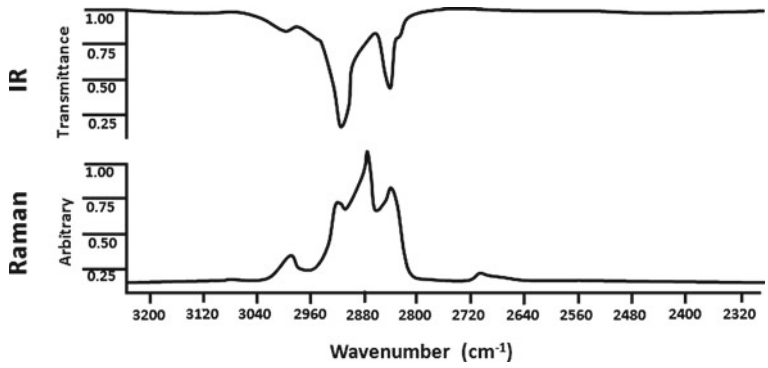

Fig. 5.4 Comparison between IR and Raman of trans-poly pentenamer

intense IR signals whereas nonpolar ones give rise to most intense Raman signals. Thus IR and Raman spectroscopy are complementary. Paired IR and Raman spectra of the same compound have a synergistic effect in promoting understanding of structural information [4].

Raman is most responsive to symmetrical stretching in C–C bonds. It is useful to study the *conformational structure* of polymer chains by comparing spectra with those of long-chain"model" alkanes. The stereoisomers of polymer is obtained by rotation around single bonds, so the Raman can be used to study the *cis–trans* isomerism in elastomers, sulfur crosslinks in rubber, and polymer deformations. Because Raman scattering by water is negligible compared with water's intense IR absorption, Raman is particularly useful in conformational studies of biopolymers in aqueous solution. Figure 5.4 shows the comparison between IR and Raman of trans-poly pentenamer. The Raman shows more feature than that of IR due to the symmetrical structure of alkane (–C–C– at 2,900 cm^{-1}) and alkene (–C=C– at 3,000 cm^{-1}). The comparison of IR and Raman spectrum of poly(3-hexyl thiophene) (P3HT) is shown in Fig. 5.5. The symmetrical C–C stretching is dominated in the Raman spectrum while the C–H stretching is dominated in the IR spectrum.

The P3HT is synthesized by Grignard metathesis reaction as shown in Fig. 5.6. The yield can be higher than 70 %. The principle of metathesis synthesis will be discussed in Sect. 9.4.

5.2.4 UV-Visible Spectroscopy

Ultraviolet–visible (UV–Vis) spectroscopy is used to detect the chromophores of matter qualitatively and quantitatively when the matter undergoes $n \rightarrow \pi^*$ and $\pi \rightarrow \pi^*$ transition upon light irradiation. Because of its sensitivity ($<10^{-5}$ molar), UV–Vis spectroscopy has been particularly useful in identifying the impurities in polymers such as residual monomer, inhibitors, antioxidant, and so on. Styrene monomer in polystyrene, for example, may be determined quantitatively using

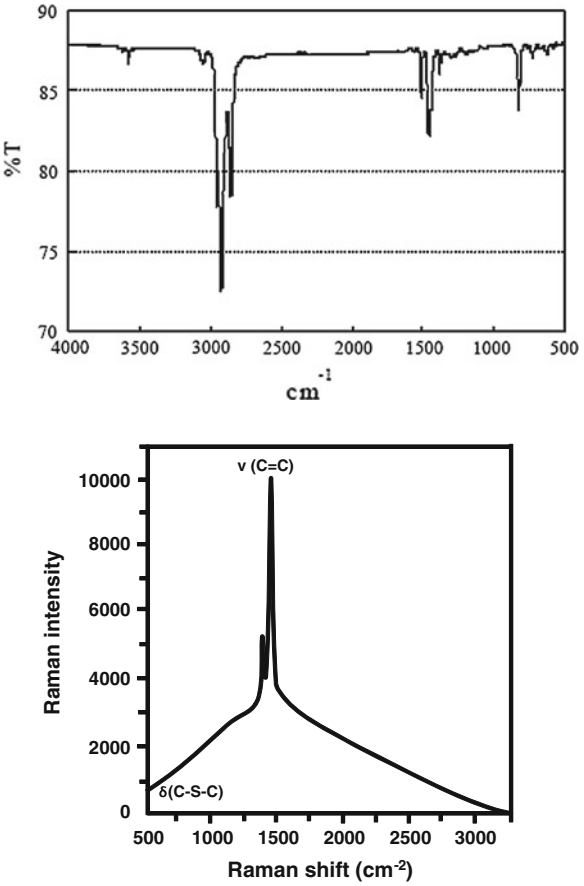

Fig. 5.5 IR spectrum (*top*) and Raman spectrum (*bottom*) of P3HT

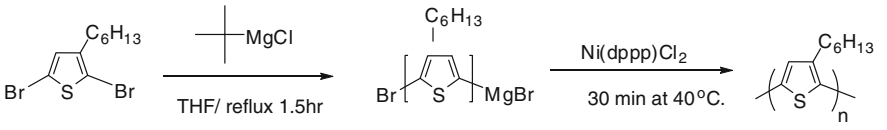

Fig. 5.6 Synthesis of P3HT using Grignard metathesis reaction

styrene's λ_{max} at 292 nm. After the styrene is polymerized, the 292 nm peak of styrene disappears and shows the λ_{max} at 203 and 254 nm of benzene for polymer.

Figure 5.7 shows a typical ultraviolet absorption spectrum of organic compound. Unlike infrared spectra, *UV–Vis spectra* are quite broad and generally show only a small number of peaks. The peaks are reported as the wavelengths where maxima occur. The conjugated, unsaturated ketone whose spectrum is shown in Fig. 5.7 has an intense absorption at $\lambda_{max} = 232$ nm and a much weaker absorption at $\lambda_{max} = 330$ nm. The band at shorter wavelength corresponds to a π

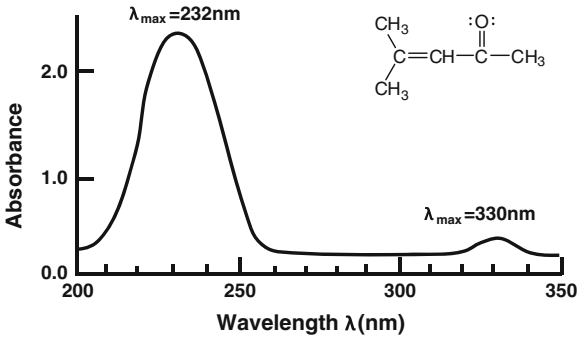

Fig. 5.7 The absorption spectrum of 4-methyl-3-penten-2-one [5]

electron transition, whereas the longer wavelength, weaker intensity band corresponds to a transition of the nonbonding electrons on the carbonyl oxygen atom.

The intensity of an absorption band can be expressed quantitatively. Band intensity depends on the particular molecular structure and also on the number of absorbing molecules in the light path. *Absorbance*, which is the log of the ratio of light intensities entering and leaving the sample, is given by Beer's law as below

$$A = \epsilon cl \tag{5.2}$$

where ϵ is the *molar absorptivity* (sometimes called the *extinction coefficient*), c is the concentration of the solution in moles per liter, and l is the length in centimeters of the sample through which the light passes. The value ϵ for any peak in the spectrum of a compound is a constant characteristic of that particular molecular structure. For example, the values of ϵ for the peaks in the spectrum of the unsaturated ketone shown in Fig. 5.7 are $\lambda_{max} = 232$ nm ($\epsilon = 12{,}600$) and $\lambda_{max} = 330$ nm ($\epsilon = 78$).

UV–Vis spectra are most commonly used to detect conjugation. In general, molecules with no double bonds or with only one double bond do not absorb in the region of UV to visible (200–800 nm). Conjugated systems do absorb there, however, and the greater the conjugation, the longer the wavelength of maximum absorption, as seen in Fig. 5.8. Therefore, most of the conjugated polymers exhibit absorption in the visible range (see Fig. 4.11).

5.2.5 Nuclear Magnetic Resonance Spectroscopy (NMR-^{1}H, ^{13}C)

The proton environment in the molecule can be determined by the nuclear magnetic resonance spectroscopy. Each proton in the molecule has its unique chemical shift δ. It is usually expressed in parts per million (ppm) by frequency. It is calculated based on the following equation:

$$\delta = \frac{\Delta\upsilon \times 10^6}{\text{oscillator frequency (cps)}} \tag{5.3}$$

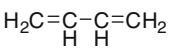

λ_{max} = 220 nm
(ϵ = 20,900)

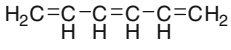

λ_{max} = 257 nm
(ϵ = 35,000)

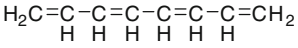

λ_{max} = 287 nm
(ϵ = 52,000)

λ_{max} = 255 nm
(ϵ = 215)

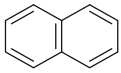

λ_{max} = 314 nm
(ϵ = 289)

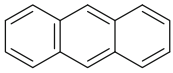

λ_{max} = 380 nm
(ϵ =9,000)

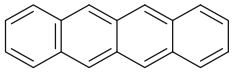

λ_{max} = 480 nm: a yellow compound
(ϵ = 12,500)

Fig. 5.8 Effect of conjugation length on the λ_{max} and ϵ of organic compounds

where $\Delta\upsilon$ is the difference in absorption frequencies of the sample and the reference in cps, and oscillator frequency is characteristic of the instrument. Chemical structures can be identified from a combination of chemical shift data and spin–spin splitting; derived from proton–proton interaction. Thus, the NMR is useful to study polymer stereochemistry and monomer sequencing. The chemical shifts of ^{1}H nuclei in various chemical environments have been determined by measuring the ^{1}H NMR spectra of a large number of compounds with known, relatively simple structures. Table 5.2 gives the chemical shifts for several common types of ^{1}H nuclei.

At present, very high resolution NMR instruments are available for polymer scientists to gain insights of polymer stereochemistry and monomer sequencing. For example, pure isotactic poly(methyl methacrylate) can have the possible arrangements for each repeat unit as shown in Fig. 5.9. By using 500-MHz NMR, a sample of poly(methyl methacrylate) has revealed to be predominantly (95 %) isotactic isomer as shown in Fig. 5.10.

The methyl protons of the sample are resolved to the pentad (*mmmm*) level and the methylene protons to the hexad (*mmmmm*) level. The notations of *e* and *t* refer to the *erythro* and *threo* placement, respectively. Of the methylene protons with respect to the ester groups, the *erythro* resonance being further downfield because of the

Table 5.2 Typical ^{1}H chemical shifts (relative to tetramethylsilane) [5]

Type	δ (ppm)	Type	δ (ppm)
C—CH$_3$	0.85-0.95	—CH$_2$—F	4.3-4.4
C—CH$_2$—C	1.20-1.35	—CH$_2$—Br	3.4-3.6
		—CH$_2$—I	3.1-3.3
C C—CH—C	1.40-1.65	CH$_2$=C	4.6-5.0
CH$_3$—C≡C	1.6-1.9	—CH=C	5.2-5.7
CH$_3$—Ar	2.2-2.5	Ar—H	6.6-8.0
CH$_3$—C(=O)—	2.1-2.6	—C≡C—H	2.4-2.7
CH$_3$—N<	2.1-3.0	—C(=O)—H	9.5-9.7
CH$_3$—O—	3.5-3.8	—C(=O)—OH	10-13
—CH$_2$—Cl	3.6-3.8	R—OH	0.5-5.5
—CHCl$_2$	5.8-5.9	Ar—OH	4-8

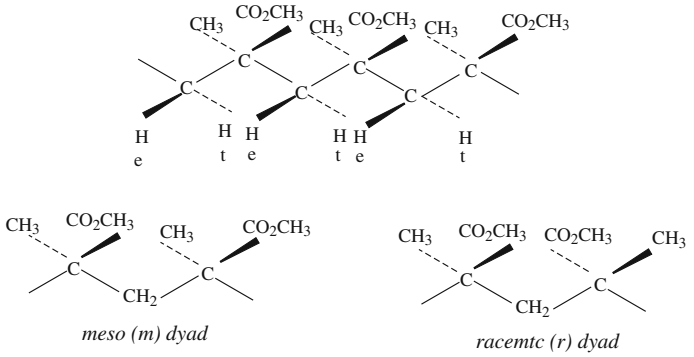

Fig. 5.9 Possible repeating unit arrangements of isotactic poly(methyl methacrylate)

deshielding influence of the ester group. At the lowest sensitivity (1X) the spectrum resembles that of almost purely isotactic (all *m*) polymer with the exception of the small *mmrm* pentad at about 1.16 ppm. At higher gain (5 and 100X), deviations from

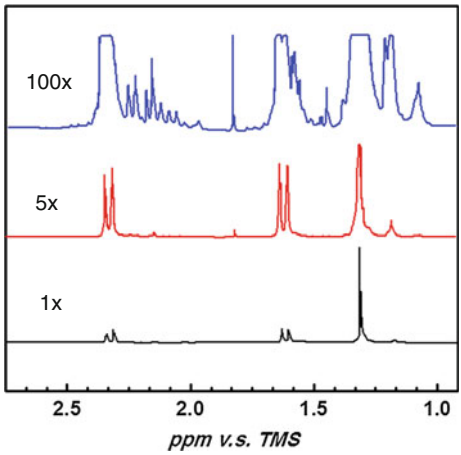

Fig. 5.10 500-MHz ^{1}H nuclear magnetic resonance spectrum of isotactic poly(methyl methacrylate). For the 1X spectrum, the *left doublet peak* is e-mmmmm, the *middle doublet peak* is t-mmmmm, the *right large singlet peak* is mmmm, the *right small singlet peak* is mmrm [3]

purely isotactic are clearly observed. On the other hand, the syndiotactic placement exhibits predominantly *racemic* (*r*) sequences at about 1.05 ppm for methyl and, because both methylene protons lie in identical magnetic environments, one singlet methylene resonance at 1.83 ppm. The methoxyl protons absorb at 3.42 ppm. Atactic poly(methyl methacrylate) would display a broad range of sequences in its NMR spectrum, in this sample, the largest peaks of impurity correspond to those of syndiotactic placement.

Figure 5.11 shows high-resolution proton-decoupled ^{13}C spectra of polypropylene of varying tacticity. Fine structure in the spectra may again be correlated with pentad sequences.

The combination of cross-polarization and magic angle spinning (CP-MAS) along with proton decoupling yields spectra of solids approaching the resolution of those obtained with solutions. As an example, Fig. 5.12 shows the solid-state ^{13}C NMR spectrum of polycarbonate with and without cross-polarization magic angle spinning, in the spectral region encompassing the carbonyl and ring carbon resonances.

5.2.6 Electron Spin Resonance

Electron paramagnetic resonance (ESR) works on the same principle as NMR except that microwave rather than radiowave frequencies are employed, and spin transitions of unpaired electrons rather than nuclei recorded. The NMR spectra record the absorption directly, but ESR spectrometers plot the first derivative of the absorption curve. The ESR in polymer chemistry is primarily for studying free radical process such as polymerization, degradation, and oxidation. For example, when poly (vinyl chloride) is irradiated with ultraviolet light, the formation of radical can be detected by ESR. The chemical reaction is shown below and its corresponding ESR spectrum is shown in Fig. 5.13.

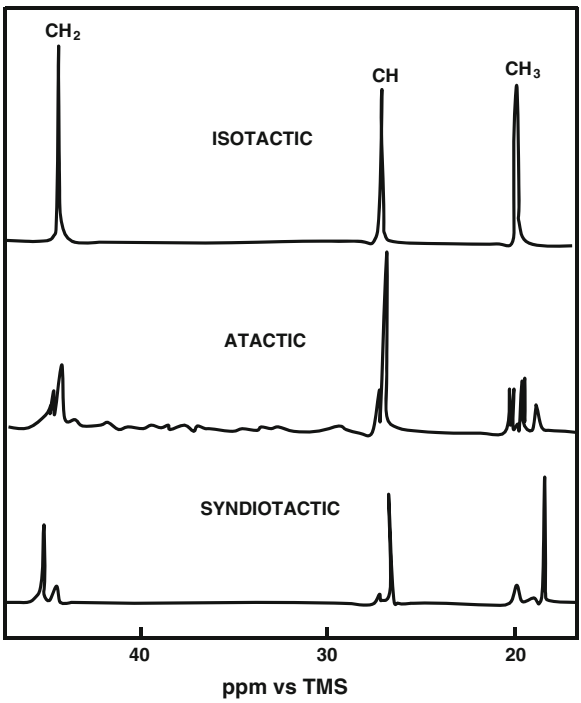

Fig. 5.11 24-MHz ^{13}C nuclear magnetic resonance spectra of polypropylene (3.5 % weight/volume in 1, 2, 4-trichlorobenzene at 135 °C) [3]

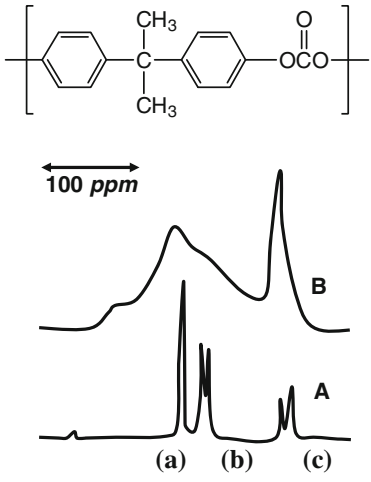

Fig. 5.12 Solid-state proton decoupled ^{13}C nuclear magnetic resonance spectra of polycarbonate (A) with and (B) without cross-polarization magic angle spinning. Peak assignment: (**a**) carbonyl carbon, (**b**) substituted ring carbons, and (**c**) unsubstituted ring carbons [3]

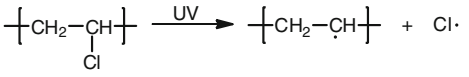

The six-line signals arise from the interaction of unpaired electron with five surrounding protons (4β and 1α). This phenomenon is called *hyperfine splitting*.

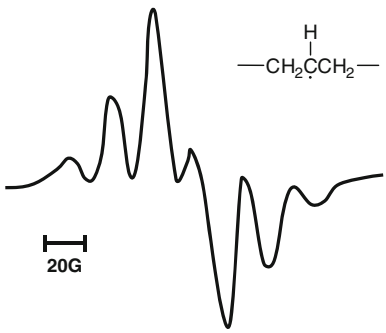

Fig. 5.13 Electron spin resonance spectrum inline of UV-irradiated poly(vinyl chloride) at −196 °C [3]

Information on the radical structure can be obtained by the line shape, intensity, position, and hyperfine splitting of the ESR spectrum.

5.3 Characterization of Morphology and Physical Structure of Polymer

Polymer morphology and structure may be elucidated from usual examination and mathematical interpretation of the pattern and intensity of diffracted and scattered X-ray, electron and neutron radiations on polymer sample. The results can provide the information of degree of crystallinity, dimension of crystalline domains, bond distance and angles, and type of conformation in the crystalline regions. Precautions need to be taken for these experiments especially involving electrons, because electrons may cause free radical reactions (chain scission, cross-linking) in the samples. Transmission electron microscopy (TEM) resolution can have up to several angstroms. Neutron scattering can study chain folding in crystalline lamellae. The AFM analyzes the surface profile of polymer thin film at nanoscale without using high vacuum and electron source.

5.3.1 Transmission Electron Microscopy

TEM is a very powerful tool to study the morphology of polymer. Here, we use the TEM study of rod-coil block copolymer of poly(diethylhexyloxy-p-phenylene vinylene)-b-poly (methyl methacrylate) (DEHPPV-b-PMMA) as an example. Figure 5.14 shows TEM images of the copolymer at various compositions. The last number in the copolymer denotations is the % volume fraction of coil PMMA [6]. The DEHPPV is a rigid rod segment and PMMA is a flexible coil segment. Due to the difference in miscibility of each segment, the copolymer is self assembled into highly ordered structure. The polymers stained with RuO_4 demonstrate light PMMA-rich nanodomains and dark DEH-PPV-rich nanodomains. Lamellae are continuous and very long. The orientation of lamellae is correlated across several

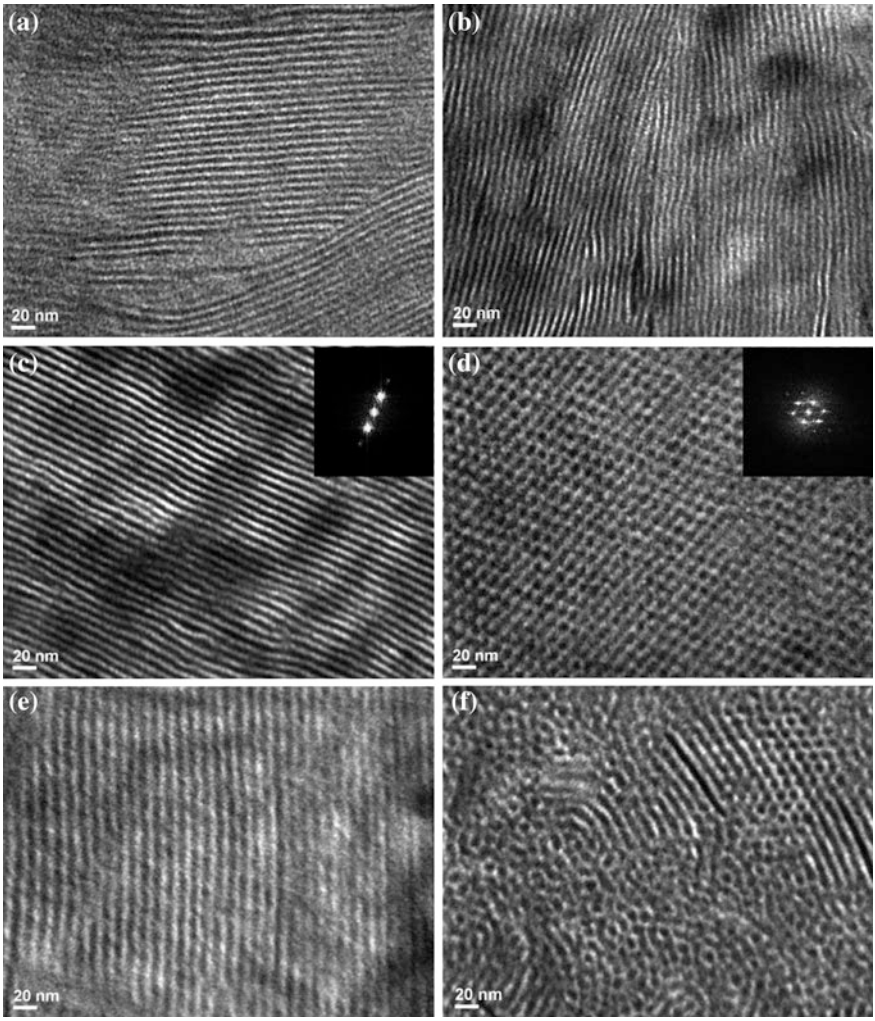

Fig. 5.14 TEM images of PPV-b-PMMA block copolymers; **a** PPV_{10}-$PMMA_{13}$-30, **b** PPV_{10}-$PMMA_{36}$-43, **c** PPV_{10}-$PMMA_{49}$-53, **d** PPV_{10}-$PMMA_{84}$-66, **e** the lateral view of PPV_{10}-$PMMA_{84}$-66, and **f** PPV_{10}-$PMMA_{126}$-74 [6]

hundreds of nanometer, or even up to a micrometer. Moreover, the lamellae have remarkable persistence length (at least several hundred nm) indicating a very high bending modulus of the DEH-PPV rod lamellar domain. Inset in Fig. 5.14c is a 2D Fourier transformation of DEH-PPV_{10}-$PMMA_{49}$-53 demonstrating the 2-fold symmetry indicative of lamellar structure and a high degree of orientation. The defects observed in the lamellae of the DEH-PPV-b-PMMA system involve curvature and T junction, with only instances of abruptly ending lamellae due to dislocations and dilations of DEH-PPV rich regions. We interpret the results as the

free energy penalty associated with additional inter-block contacts at the core of a dislocation was much higher than the bending penalty imparted by the rod rigidity. As a result, this system's higher segregation strength results in greater lamellar continuity and a greater presence of curvature defects instead of lamellar breaks.

TEM images of the more asymmetric block copolymers (i.e., volume fraction of copolymer is apart from 50 %), as shown in Fig. 5.14d, show that the DEH-PPV rods are packed into short strip-like aggregates assembled onto a hexagonal lattice. Moreover, the 2D Fourier transformation inset in Fig. 5.14d has 6-fold symmetry indicative of the hexagonal structure with high degree of orientation. The lateral view of the polymer is also investigated by tilting the sample. TEM image, as shown in Fig. 5.14e, shows that alternating stripes with light and dark are observed. However, the stripes in the hexagonal structure are shorter than the stripes in the lamellar polymers. The short strip-like aggregates with the hexagonal packing appear again, while the lamellae across the boundary. In summary, in asymmetric copolymers, the DEH-PPV rods pack into hexagonally arranged strips. These strip aggregates are much longer in the third dimension than the two small dimensions.

TEM image gives complementary information for the block copolymer with coil volume fraction at 74 %, as shown in Fig. 5.14f. Short strip-like aggregates and longer strip-like aggregates with intermediate orientational order still can be observed. As compared to the structure of DEH-PPV_{10}-$PMMA_{64}$-66, the structure of DEH-PPV_{10}-$PMMA_{126}$-74 is similar to the hexagonal structure.

5.3.2 X-Ray Scattering

X-ray technique is the most important method to determine the spatial arrangements of all the atoms in polymers [3]. X-rays are generated in cathode ray tubes when high energy electrons impinge on metal target such as copper. When X-rays are focused on a polymer sample, two types of scattering occur. If a sample is crystalline, the X-rays are scattered coherently; that is, there is no change in wavelength or phase between the incident and scattered rays. Coherent scattering is commonly referred to as X-ray diffraction. If the sample has a nonhomogeneous (semicrystalline) morphology, the scattering is incoherent; there is change in both wavelength and phase. Incoherent scattering is referred to as diffuse diffraction or simply as scattering.

Coherent scattering is determined by wide-angle measurements and incoherent scattering by small angle measurements as shown in Fig. 5.15. The former is called wide-angle X-ray scattering (WAXS) and the latter is named small-angle X-ray scattering (SAXS). The wide angle diffraction pattern consists of a series of concentric cones arising from scattering by the crystal planes. It is recorded as concentric rings on the X-ray plate superimposed on a diffuse background of incoherent scatter as shown in Fig. 5.15. On the contrary, small-angle scatter patterns are very diffuse (Fig. 5.15). Another way to present the two dimensional scattering spectrum of the polymer is making a plot of intensity versus angle of scattering. The patterns and intensity of X-ray scattering can provide considerable

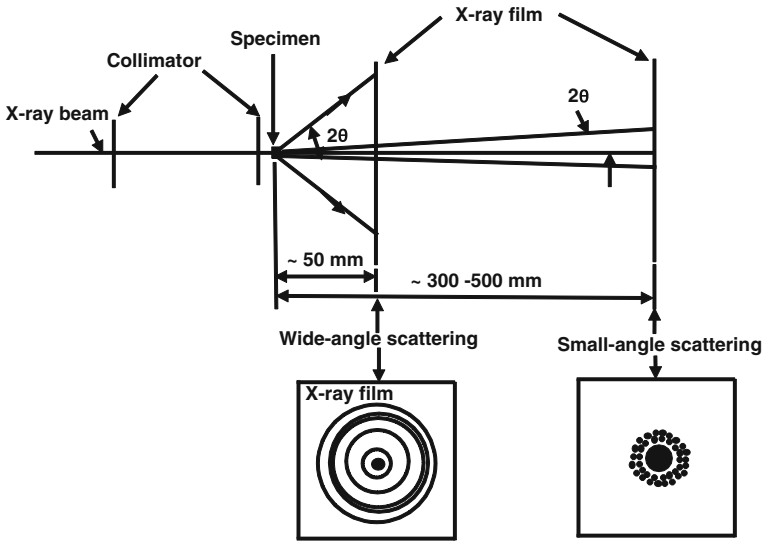

Fig. 5.15 Wide-angle and small-angle X-ray scattering techniques [3]

information regarding the polymer morphology and structure through visual examination and mathematical modeling interpretation. Examples of scattering patterns of P3HT-b-P2VP copolymer and P3HT were discussed earlier in Sects. 3.3 and 3.8, respectively.

5.3.3 Atomic Force Microscopy

Atomic force microscopy (AFM) is used to monitor the surface roughness and hardness of polymer; phase separation of polymer blends. The essential features of AFM are shown in Fig. 5.16. The atomic scale probe is scanned through the

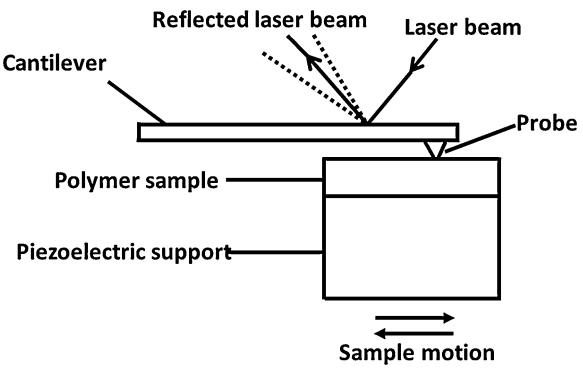

Fig. 5.16 Schematic diagram of an atomic force microscope [3]

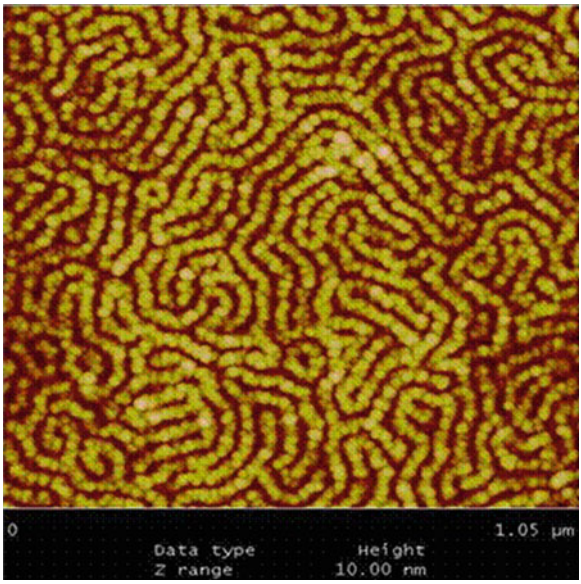

Fig. 5.17 AFM image of PS-b-PMMA

surface of sample, the change in depth is monitored by laser beam irradiated on the cantilever, fed back by piezoelectric force that response to surface variations sensed by the probe. The sample is mounted on the piezoelectric support. Figure 5.17 shows the phase separation of polystyrene and poly(methyl methacrylate) diblock copolymers (PS-b-PMMA) on glass substrate. The light color image is PS and the dark color image is PMMA. The PS has a higher depth profile and is toward air because of its hydrophobic characteristics.

5.4 Characterization of Thermal Properties of Polymers

Thermal analysis is used to study the thermal stability, melting point, glass transition temperature (Tg), and flammability, etc. The methods include DTA, DSC, DMA, TMA, and TGA. The full name and principle of each method is described in the following sections.

5.4.1 Differential Thermal Analysis and Differential Scanning Calorimetry

Before the invention of DSC, the differential thermal analysis (DTA) is commonly used to determine the thermal stability of polymer. The DTA, both sample and reference are heated by the same heat source and the difference in temperature ΔT between the two is recorded. When a transition occurs in a sample, a temperature

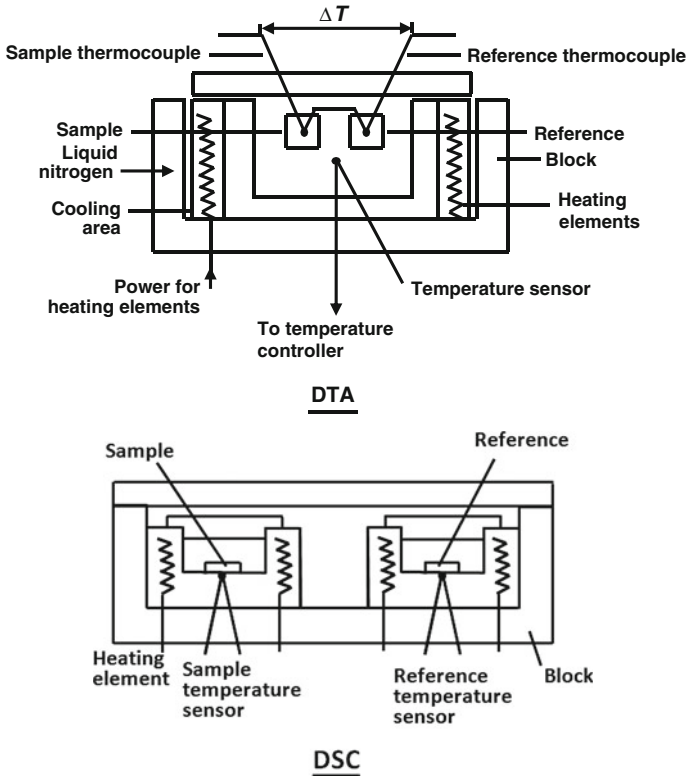

Fig. 5.18 Schematic illustrations of DTA and DSC measuring cells [3]

lag will show as endothermic or exothermic depends on the transition. For DSC, sample and reference are provided with individual heaters, and energy is supplied to keep the sample and reference temperatures constant. The electrical power difference between sample and reference is recorded as dΔQ/dt. Schematic representations of DTA and DSC cells are given in Fig. 5.18. The DTA data only report the softening (phase transition) temperature of polymer while the DSC also provide the amount of heat involved in the softening process. The DSC is more preferred in the polymer characterization because the precise control and measurement of heat varied in the heating process.

Data are plotted as ΔT (for DTA) or dΔQ/dt (for DSC) on the ordinate against temperature on the abscissa. Such plots are called *thermograms*. Although ΔT and dΔQ/dt are not linearly proportional, they are both related to heat capacity. Thus, DSC and DTA thermograms have the same form. An idealized DSC or DTA thermogram for a hypothetical crystallizable polymer is depicted in Fig. 5.19. The figure shows the types of transitions that are interested to polymer scientists.

In reporting transition temperatures, it is important to indicate whether one is referring to the onset of the transition or to the inflection point peak maximum, as shown in Fig. 5.20. Both conventions are used.

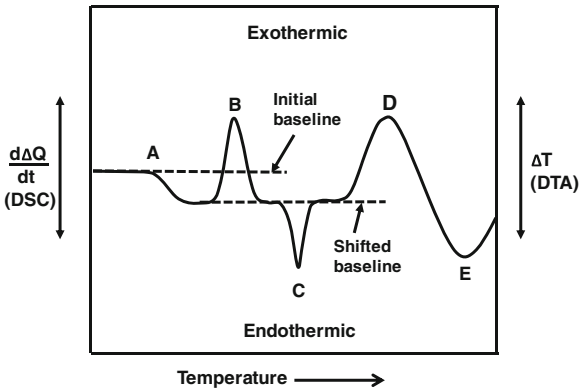

Fig. 5.19 Idealized differential scanning calorimetry (DSC) or differential thermal analysis (DTA) thermogram: (A) temperature of glass transition, T_g; (B) crystallization; (C) crystalline melting point, T_m; (D) crosslinking; and (E) vaporization. dΔQ/dt is the electrical power difference between sample and reference; ΔT is the difference in temperature between sample and Ref. [3]

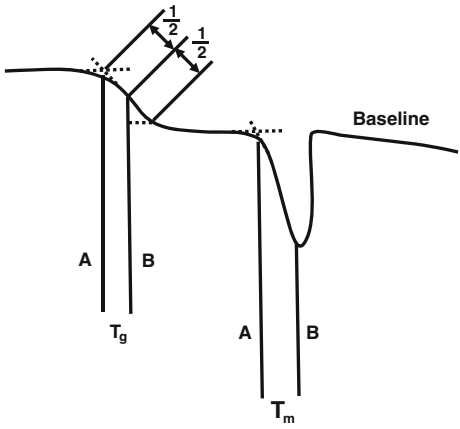

Fig. 5.20 Methods of reporting transition temperatures: (A) at the onset, and (B) at the inflection point or maximum. T_g = glass transition temperature. T_m = crystalline melting point [3]

5.4.2 Thermomechanical Analysis (TMA)

TMA employs a sensitive probe in contact with the surface of a polymer sample under a defined load. As the sample is heated, the probe senses thermal transition such as T_g or T_m by detecting either a change in volume or a change in modulus. TMA is generally more sensitive than DSC or DTA for detecting thermal transitions, especially for thermoset because the TMA probe is in direct contact with the sample. Figure 5.21 shows bisphenol epoxy resin (BP) was cured with phenolic resin (PF5110) and the thermoset transition occurred at 150 °C [7].

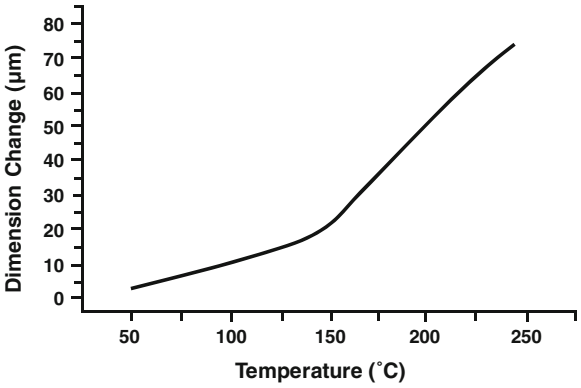

Fig. 5.21 Thermomechanical analysis of phenolic resin (PF5110) cured epoxy resin (BP) [7]

5.4.3 Thermogravimetric Analysis

Thermogravimetric analysis (TGA) is used primarily for determining thermal stability of polymers. The most widely used TGA method is based on continuous measurement of weight on a sensitive balance (called a *thermobalance*) as sample temperature is increased in air or in an inert atmosphere. Data are recorded as a weight loss versus temperature. A typical thermogram illustrating the difference in thermal stability between a wholly aromatic polymer and a partially aliphatic polymer of analogs structure is shown in Fig. 5.22.

Fig. 5.22 Thermogram of thermogravimetric analysis of polythiazoles [3]

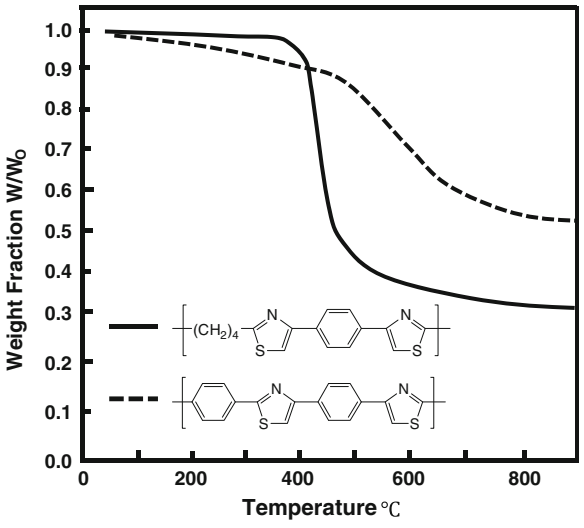

5.4.4 Flammability Test

Flammability is difficult to measure because the result does not correlate directly the burning behavior in true fire conditions of polymer. Currently, the *limiting oxygen index* (LOI) of polymer is employed as an indication of flammability of polymer. The LOI is the minimum percentage of oxygen in an oxygen–nitrogen mixture that will initiate and support for three minutes the candle like burning of a polymer sample; that can be expressed by Eq. 5.4. The test can be easily carried out in the laboratory using a small-scale fire.

$$\mathrm{LOI} = \frac{\mathrm{vol.}\, O_2}{\mathrm{vol.}\, O_2 + \mathrm{vol.}\, N_2} \times 100 \tag{5.4}$$

Representative LOI values for some common polymers are given in Table 5.3. Note the large difference in LOI between poly(ethylene oxide) and poly(vinyl alcohol), although they have similar structure. The dehydration of polyvinyl alcohol will cool the polymer during burning. The polymers contained ether linkage exhibit low LOI due to the presence of oxygen atom. Although the polycarbonate contains oxygen, it releases fire extinguishing CO_2 during burning which increases the LOI value. The polymers having aromatic structure especially in the backbone show high LOI, because the aromatic chain is more difficult to break and burn than that of alkyl chain such as poly(phenylene oxide). The inclusion of Si in the polymer increases the LOI because Si is nonflammable as compared to C. The chloride bond of polyvinyl chloride is easy to break under heat and function as an extinguisher to reduce the burning which results in high LOI. The poly(tetrafluoro ethylene) exhibits the highest LOI among the polymers because of the strong C–F bonding and dense structure of the polymer.

Table 5.3 Limiting oxygen indexes (LOI) of some common polymers [3]

Polymer	LOI
Poly(oxy methylene)	15
Poly(ethylene oxide)	15
Poly(methyl methacrylate)	17
Polypropylene	17
Polyethylene	17
Polystyrene	18
Poly(1,3-butadiene)	18
Poly(vinyl alcohol)	22
Polycarbonate	27
Poly(phenylene oxide)	28
Polysiloxane	30
Poly(vinyl chloride)	45
Poly(vinylidene chloride)	60
Poly(tetrafluoro ethylene)	95

5.5 Problems

1. A copolymer of propylene and vinyl chloride contains 35wt. % chlorine. What is the molar ratio of vinyl chloride to propylene in the copolymer?
2. What kind of polymer can you deduce from the following IR spectrum?

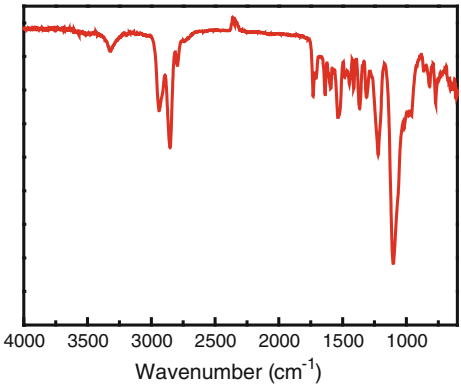

3. One stereoregular form of polystyrene (A) has a ^{1}H NMR spectrum containing a triplet centered at about 1.4 ppm and a quintet at about 1.9 ppm. Another stereoregular form (B) has an octet at about 1.6 ppm. Interpret the spectra and determine which corresponds to isotactic and which to syndiotactic.
4. How would you distinguish between the following two polymers by IR and NMR?

$$[\mathrm{p{-}C_6H_4{-}CH_2}]_n{-},\ {-}[\mathrm{o{-}C_6H_4{-}CH_2}]_n{-}$$

5. What changes would be observed in the XRD patterns of rubber that has been stretched?
6. Please use a spectroscopic method to determine the following and explain your answer. (a) The amount of styrene in a styrene-butadiene copolymer. (b) The amount of 1,2- polymer in poly(1,3-butadiene). (c) The stereochemistry of double bonds in 1,4-poly(1,3-butadiene). (d) Unreacted polyacrylonitrile (PAN) is present in a sample of carbon fiber prepared by pyrolysis of PAN. (e) Poly(vinyl acetate) has undergone hydrolysis on exposure to moisture. (f) A polyester surgical implant has been coated with polyterafluoroethylene completely to improve its chemical resistance.
7. Which technique would you use to solve the following problems, (a) locate a crystalline melting temperature, (b) determine the degree of orientation, (c) determine the arrangement of molecular chains in a polymer crystal, (d) locate the glass transition temperature, (e) characterize the double bond in the diene polymer, (f) measure the enthalpy of fusion, (g) investigate the mechanism of oxidation of a polymer, (h) study the molecular motion of polymer chains, (i)

estimate the degree of crystallinity, (j) measure the amide content of an ester-amide copolymer.

8. Show how NMR can be used to (a) distinguish between head-to-head and head-to-tail polymerization in polymer, (b) distinguish between a random copolymer and a mixture of homopolymers.
9. Draw typical DSC and DTA thermograms for a crystalline polymer, showing the glass transition, crystallization, crystalline melting and thermal degradation.
10. Please answer the following questions:

    (a) Which of the following aromatic compounds do you expect to absorb at the longer wavelength?

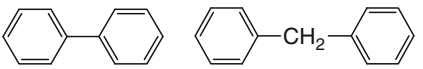

    (b) Naphthalene is colorless, but its isomer azulene is blue. Which compound has the lower-energy pi electronic transition?

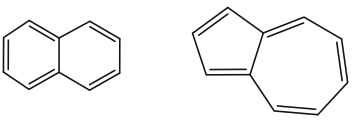

naphthalene azulene

    (c) Does the molecular weight affect the absorption wavelength (λ_{max}) of polymer? Please compare the difference of UV–Vis spectrum of polythiophene between molecular weight of 3000 and 30,000. Explain your answer.

References

1. N.M. Bikales (ed.), *Characterization of Polymers* (Wiley-Interscience, New York, 1971)
2. J.R. Dyer, in *Applications of Absorption Spectroscopy of Organic Compounds* (Prentice-Hall, Inc., Eagle-wood Cliffs, 1965)
3. M.P. Stevens, *Polymer Chemistry*, 3rd edn. (Oxford University Press, New York, 1999)
4. A.H. Kuptsov, G. N. Zhizhin, in *Handbook of Fourier Transform Raman and Infrared Spectra of Polymers* (Elsevier Science B.V., Amsterdam, 1998)
5. H. Hart, L. Craine and D. Hart, *Organic Chemistry*, 7th edn. (Houghton Mifflin Company, Boston, 2003)
6. C.C. Ho, Y.H. Lee, C.A. Dai, R. Segalman, W.F. Su, Macromolecules **42**(12), 4208–4219 (2009)
7. D. Lee, Master Thesis of National Taiwan University, (Taipei, Taiwan, 2001), 64